Hindawi
Geofluids
Volume 2021, Article ID 6694532, 12 pages
https://doi.org/10.1155/2021/6694532

Research Article

Interrelationships between Acoustic Emission and Cutting Force in Rock Cutting

Sifei Liu,[1,2,3] Peng Shi,[1,2] Zhijun Wan,[1,2] Shuaifeng Lu,[1,2] Jiakun Lv,[1,2] and Fanfei Meng[3]

[1]*School of Mines, China University of Mining and Technology, Xuzhou 221116, China*
[2]*Key Laboratory of Deep Coal Resource Mining (CUMT), Ministry of Education of China, China*
[3]*Department of Earth Resources Engineering, Faculty of Engineering, Kyushu University, Fukuoka 819-0395, Japan*

Correspondence should be addressed to Zhijun Wan; zhjwan@cumt.edu.cn

Received 25 November 2020; Revised 14 January 2021; Accepted 5 February 2021; Published 24 February 2021

Academic Editor: Weijun Shen

Cutting force is the key signal to realize intelligent control of shearer and mastering the change process of cutting force is helpful to improve the adaptive cutting of shearer. In this paper, full scale rock cutting tests are used to carry out single pick cutting experiments on three kinds of coal, and the acoustic emission (AE) signals of coal and rock cutting are monitored in the whole process. The relationship between AE and cutting force is also discussed. The results show that the development of AE energy can represent the different stages of the cutting process, and the time fractal dimension of AE energy can reveal the change law of coal structure stability. In addition, the acoustic emission waveform at the peak cutting force of the same kind of coal has the same main frequency, power spectrum density (PSD) variation law, and the area under PSD curve; for different types of coal, the area under PSD curve at peak cutting force increases with the increase of USC. In the cutting process, the AE signal has obvious characteristics and internal evolution law in energy amplitude, fractal dimension, and PSD index. The change characteristics of AE energy can be used as the precursor information of the peak cutting force, and the coal failure at the peak cutting force has the identity. The above conclusions are of great significance for intelligent control of shearer and intelligent mining of coal mine.

1. Introduction

In recent years, mining machinery and equipment have been greatly developed, and the mining efficiency has been improved. The cutting force is the power source in the process of coal cutting, and it is an important basis for the design of mining machinery. It has been a hot spot for scholars. Many scholars have carried out in-depth research on the cutting force by experimental research [1–5], numerical simulation [6–9], and microscopic analysis, proposing different cutting force models to explain the rock failure mechanism. However, the cutting force has been dynamically changing during the cutting process and the changing process is complicated, which makes it difficult to grasp the change of the cutting force in real time. As shown in Figure 1, the typical cutting force curve is a jump-in type with multiple peaks. At the same time, the peak cutting force is the most important factor in mining machinery selection, design, and improvement of the reliability of mining machinery. Therefore, many scholars turn to the study of peak cutting force. Scholars establish a cutting force model to predict peak cutting force by tensile failure criteria [10–13] and fracture mechanics [14–16]. Some scholars also pay attention to the average peak cutting force [16] and establish a mechanical model to predict the average peak cutting force. The above results of the study have greatly promoted the development of mining machinery and gradually developed towards intelligence. The intelligent mining of mines has been widely recognized by the academic community and the industry. Real-time intelligent perception of the production environment is the basic requirement for intelligent control of mining machinery. It requires real-time analysis of the cutting force to achieve intelligent control of the cutting machine in terms of cutting speed, traction speed, and cutting height. However, few scholars have paid attention to the variation characteristics of the cutting force during the rock cutting process, and

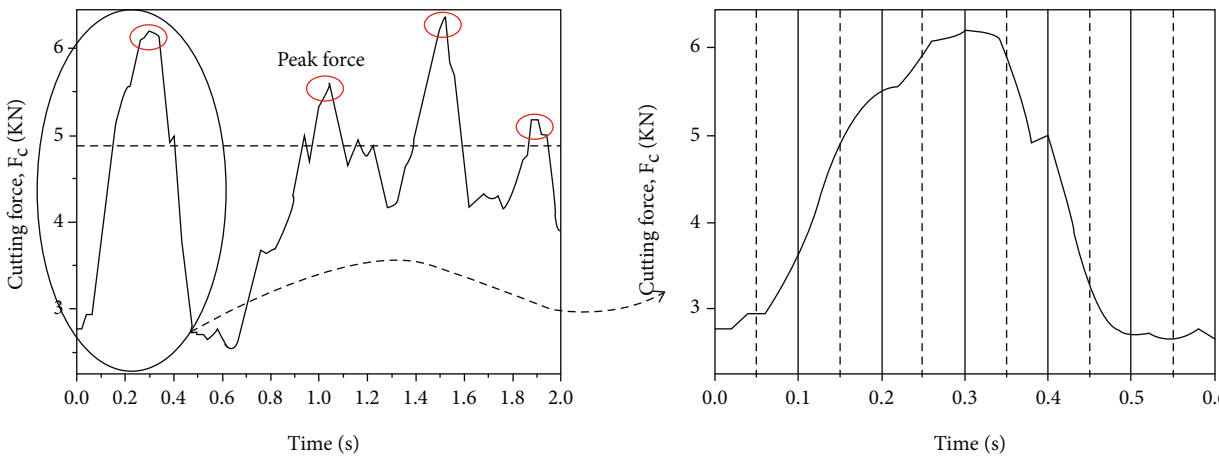

Figure 1: The typical cutting force curve of coal-cutting.

there is no report on the prediction of the peak cutting force occurrence time. In recent years, the introduction of variable frequency motor into mining equipment requires real-time analysis of cutting force to avoid the occurrence of peak cutting force, reduce the fatigue damage of the pick, achieve balanced cutting, and improve the reliability of mining equipment. Therefore, it is necessary to strengthen the grasp of the cutting force process, and timely predict the arrival of peak cutting force through technical means.

Acoustic emission technology is an online monitoring method that detects, locates, and characterizes the damage and destruction characteristics of metal and rock materials. In early rock cutting studies, rock acoustic emission waveforms and spectra have been shown to be sensitive to abnormal conditions in cutting, with different rocks having different acoustic emission frequencies [17]. Table 1 shows the prerock interception acoustic emission data, including rock categories, conclusions, and data analysis methods. Acoustic emissions contain a portion of the elastic energy released by microscopic deformation, including dislocation motion, crack propagation, and erosion. In addition, AE energy is theoretically proportional to the energy released by rock rupture [18]. Power spectral density is an important indicator for quantifying acoustic emission energy [19, 20]; however, the target materials discussed in the study are mainly metals or composites, as shown in Table 1. Further, different rocks have different acoustic emission characteristics, and coal as a biogenetic organic mineral rock has a soft texture and allows large deformation, which is more specific for cutting. Therefore, there is no extensive and in-depth study on the acoustic emission characteristics of coal cutting.

In this paper, the acoustic emission experimental study of single-tooth cutting is carried out, and the correlation between the cutting force of 3# coal (H_2 coal) and acoustic emission energy in Baigou Coal Mine is discussed. At the same time, the precursor of the peak cutting force is analyzed by the development of time fractal dimension of acoustic emission energy. In addition, this paper analyzes the power spectral density and energy of the acoustic emission waveform at the peak cutting force. All of these are to find the commonality of different peak cutting forces and to find the sign of peak cutting force, which will provide the basic parameters for the intelligent control of mining machinery.

2. Experiment Apparatus

2.1. Experimental Setup. To collect the acoustic emission data of coal-cutting, a series of Full-scale Rock Cutting Testing Machine were carried out with a full-scale linear rock cutting tester. The schematics of the cutting tester are shown in Figure 2(a). It can accommodate rock samples up to 700 × 700 × 1000 mm^3 in size. The three-dimensional (3D) forces acting on the pick can be recorded by a 3D force sensor up to 50 tons. The data sampling rate is adjustable up to 1 MHz. The pick used in this cutting testing machine is a U135-25 conical pick with a tip angle of 90° and a tip diameter of 25 mm. A cutting speed of 0.075 m/s, an attack angle of 55°, and a rake angle of 10° are used in these tests. The sampling rate of cutting force is 2000 Hz.

An eight-channel AE acquisition system with a high sampling rate of 3 MHz and 40 dB preamplification was used to record the AE data generating from the rock fragmentation. The acquisition band of the acoustic emission probe is 200-400 kHz. The acoustic emission probe is attached to the surface of the sample, four on each side, symmetrically distributed, as shown in Figure 2(b). After the probe is pasted, the sound wave velocity in the sample is calibrated using the sound emission system's own software.

2.2. Materials and Procedures. In this paper, three types of coal were used to study the characteristics of cutting force and acoustic emission. The coal samples were from Maodi Mine 13# coal, Baigou Coal Mine 3# coal, and Shuozhou surface coal mine, labeled L_1, H_2, and H_3. According to the ISRM regulations, relevant mechanical experiments were carried out to determine the physical and mechanical parameters of three types of coal, as shown in Table 2.

The sample was cut from the intact large coal sample in the field and polished into a smooth and flat cube test piece, the size of which is 400 × 300 × 150 mm^3. In this process, the secondary

Table 1: Summary of earlier acoustic emission monitoring studies of rock-cutting.

Authors	Materials	Work and results	AE processing methods
Ma 1996 [17]	Limestone, granite, diorite, marl, etc.	Different rocks have different acoustic emission frequencies.	Not described
Kovacevic 1998 [20]	Magnesia chromite, sintered magnesia, bauxite	RMS of AE was investigated to establish the function of drilling depth for the study of material (metal) removal mechanisms.	Fast Fourier transform (FFT); PSD by using autoregressive moving average(ARMA) model
Momber 2000 [21]	Concrete materials	Integrated AE technique and visualization method to monitor erosion process of concrete material.	FFT and frequency domain analysis
Kovacevic 2002 [22]	Gray cast iron	Proposed an energy dissipation model and interpreted the relations of AE signal with energy dissipation.	PSD by using ARMA model; FFT and frequency domain analysis
Karakus 2014 [23]	Hard rock	Make it possible to estimate the depth of cut, weight on the bit (WOB), and torque on the bit (TOB) by simply using the time spectrum of the AE signals.	FFT and frequency domain analysis
Xiao 2018 [24]	Concrete	Spectral analysis of the AEs indicated that the higher ROP and larger cutting size were correlated with a higher AE energy and a lower AE frequency.	FFT and frequency domain analysis

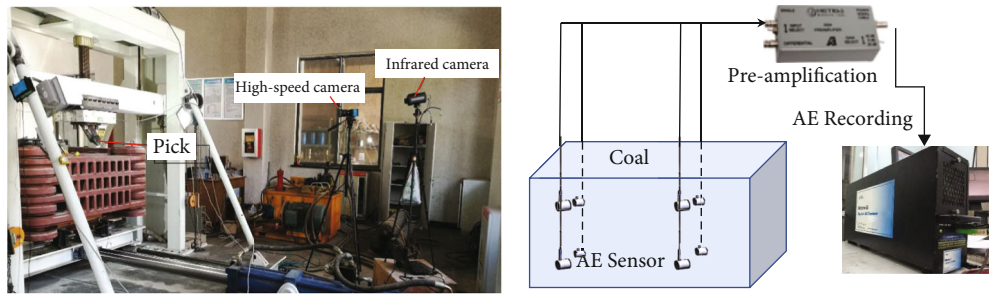

(a) Schematics of the full-scale rock cutting tester (b) An eight-channel AE acquisition system

Figure 2: A schematic of the experimental setup.

Table 2: Mechanical properties of the samples.

Sample	UCS/MPa	BTS/MPa	KIC/(MPa·m$^{1/2}$)
C1	4.24 ± 1.47	0.72 ± 0.23	0.132
C2	6.68 ± 3.63	0.81 ± 0.49	0.169
C3	9.64 ± 2.81	1.14 ± 0.15	0.229

physical and chemical damage of the sample is minimized. After the sample was processed, the sample was packaged into a test piece having a size of 400 × 600 × 200 mm^3 with a concrete material and was used for seven days after curing.

3. Evolution Characteristics and Correlation Analysis of Acoustic Emission and Cutting Force

3.1. Amplitude Evolutionary Process of the AE Energy. The acoustic emission energy can represent the density and intensity of acoustic emission activity [25]. Taking H_2 coal as an example, the change trend of acoustic emission energy during the whole cutting experiment is shown in Figure 3(a). It was found that there was a cluster of acoustic emission energy at a large cutting force, but the amplitude of the acoustic emission energy differed greatly, which resulted in the inability to display local details. Therefore, in the article, the number of acoustic emission energy is taken as $\log_{10}$, and Figure 3(b) is obtained. It is found that the acoustic emission energy and the cutting force change periodically with time. On the whole, the acoustic emission energy appears clustering at the peak of the cutting force, and the number of acoustic emission is large and the energy is large, which indicates that the coal body has a large number of damages and the damage intensity is large. Where the cutting force is small, the acoustic emission has a low density and low energy, indicating that although the coal body is damaged, the breaking strength is low. Therefore, the acoustic emission energy has a correlation with the cutting force. According to local analysis, coal cutting can be divided into three stages: compaction stage, stable extrusion stage, and large particle stripping in a single cycle. As shown in Figure 4(c), at the beginning of the cutting, the cutting force is small, the coal sample is in the compacting stage, the microcracks are gradually closed, the acoustic emission density is large, and there is a certain energy. As the cutting force gradually increases and enters the stable extrusion stage, the coal begins to undergo large deformation, small debris is generated, the

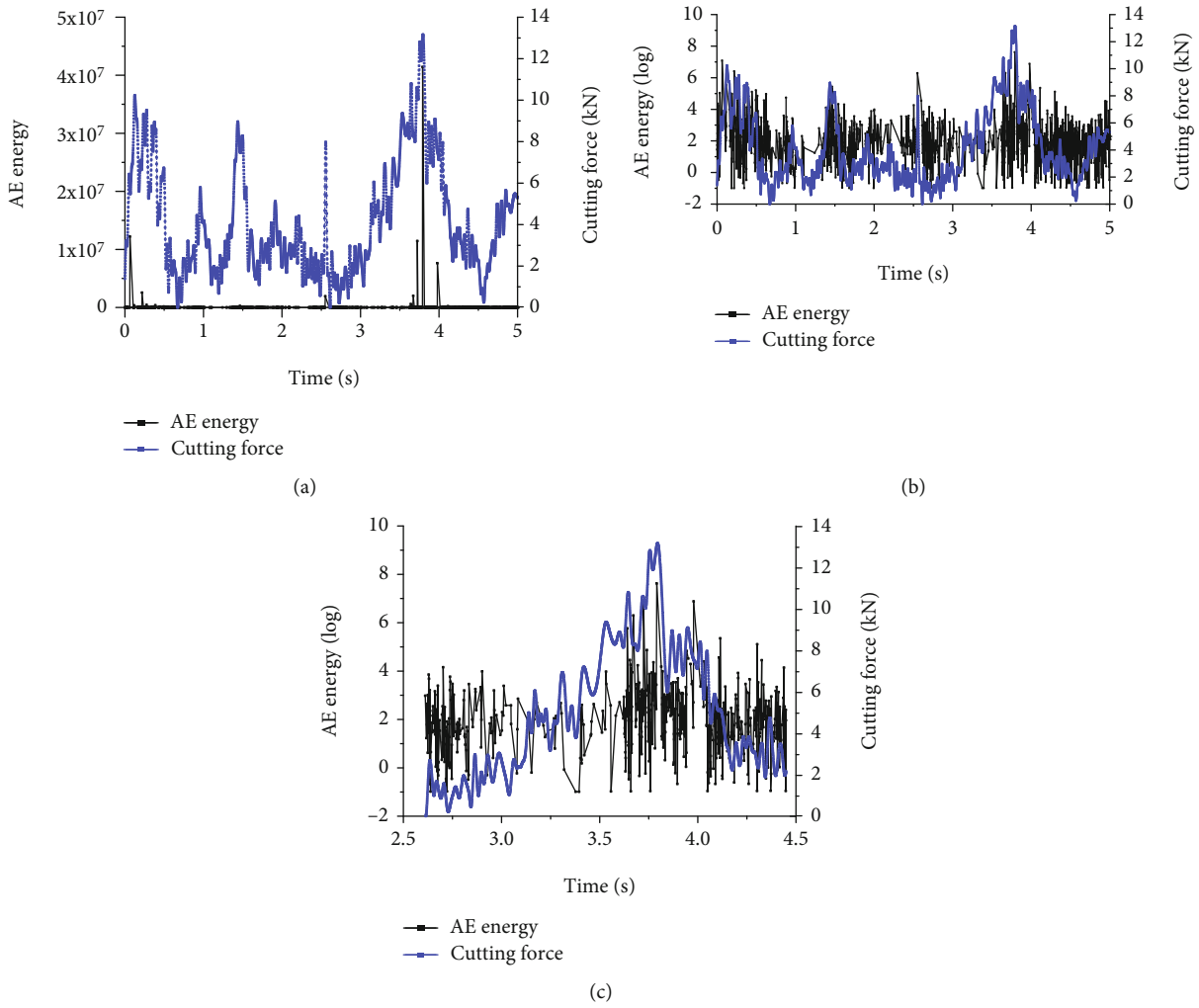

FIGURE 3: H_2 coal cutting acoustic emission energy.

number of acoustic emission occurs less, and the energy is less, showing a "relatively quiet period". However, when the cutting force reaches the maximum value and the cutting enters the bulk particle size stripping stage, the number of acoustic emission occurrences increases sharply, and the energy also reaches the maximum value. The acoustic emission energy shows a strong correlation with the cutting force, and the development of the acoustic emission energy can characterize the different stages of cutting.

3.2. AE Fractal Evolutionary Process. Studies have shown that acoustic emission signals have temporal fractal characteristics during rock failure [26–28]. According to the fractal geometry theory of fractal geometry and acoustic emission, the calculation formula of the correlation integral $C(t)$ of the amplitude distribution of acoustic emission signals over time during rock rupture [26, 28] is

$$C(t) = \frac{2M(t)}{M(M-1)}, t \le T, \quad (1)$$

where T is the total time course, t is the time interval between the amplitudes during T time, $M(t)$ is the logarithm of the sum of the amplitudes in time t, and M is the amplitude in the range of T time sum.

The time fractal dimension D_t of the magnitude [28] is

$$D_t = \lim_{t \to T} \frac{\lg C(t)}{\lg t}. \quad (2)$$

It can be seen from the above formula that fractal dimension D_t increases, indicating that the rate change in a period of the acoustic emission signal energy is larger, corresponding to larger strength damage. Conversely, the smaller the time fractal dimension D_t is, the smaller the corresponding strength will be.

Figure 4 shows the time fractal dimension of acoustic emission energy during H_2 coal cutting, with the following characteristics:

(1) The change process of time fractal D_t value is in good agreement with the evolution process of cutting force. The maximum value of D_t appears at the point of peak cutting force, indicating that the coal body has a large damage at the peak

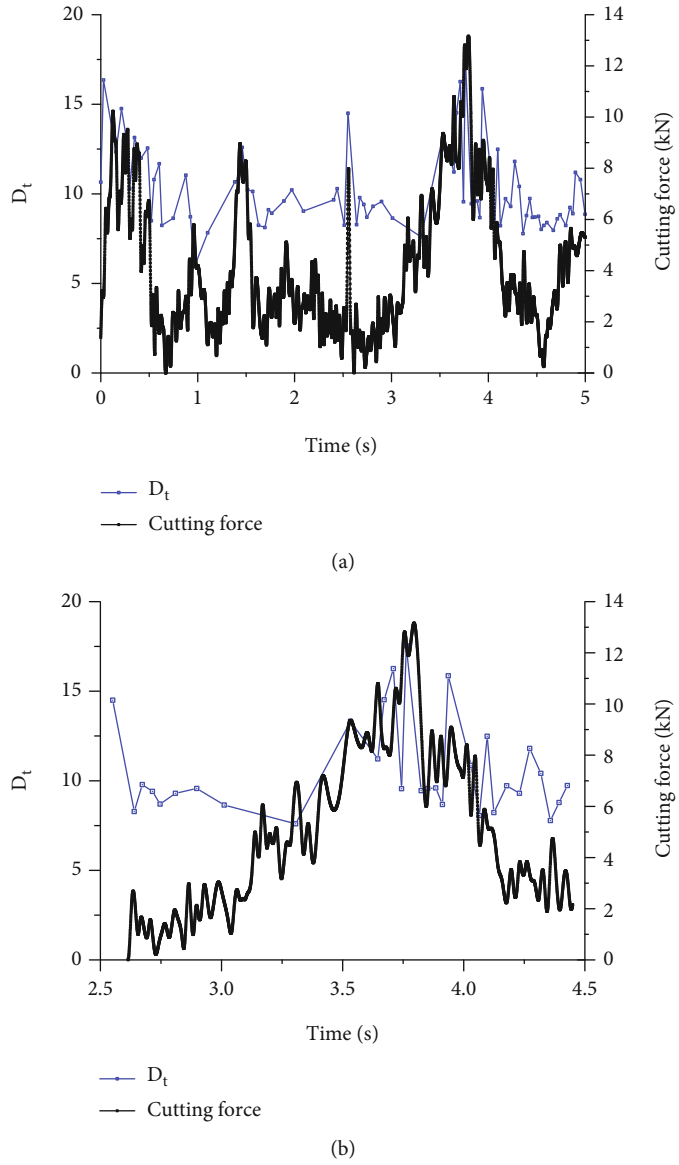

Figure 4: Time fractal dimension of acoustic emission energy of cutting H_2 coal.

cutting force and the rate of D_t change is large, which is consistent with the actual situation. In other cutting stages, the cutting force is small and the D_t value is relatively stable, indicating that the cutting damage is relatively small

(2) For a single cutting cycle, the time fractal D_t can also be divided into three stages, namely the steady phase, the rising phase, and the falling phase. In the stable phase, the D_t value has a downward trend but does not reach 0, showing that there is a relatively stable acoustic emission in the coal body, and the cutting force is small, which means that there are more microcracks closing, and gradually develop to a stable structure. During the ascending phase, the D_t increases rapidly, indicating that the coal body gradually develops toward unstable structures, and when the D_t reaches the peak, the coal body undergoes large damage. In the stage of rapid decline of D_t, it indicates that the coal gradually develops to a stable structure after major damage

(3) The time of the cutting process in Figure 4(b) is 1.78 s, and the times of compaction phase, stable extrusion phase, and bulk particle stripping phase are 0.51 s, 0.49 s, and 0.78 s, respectively. The cut-off time from the end of the stable extrusion to the peak cutting force is 0.09 s

In summary, the time dimension of acoustic emission has a good correlation with the cutting force. Before the peak cutting force, the D_t value increases rapidly and reaches a peak at the peak cutting force. In combination

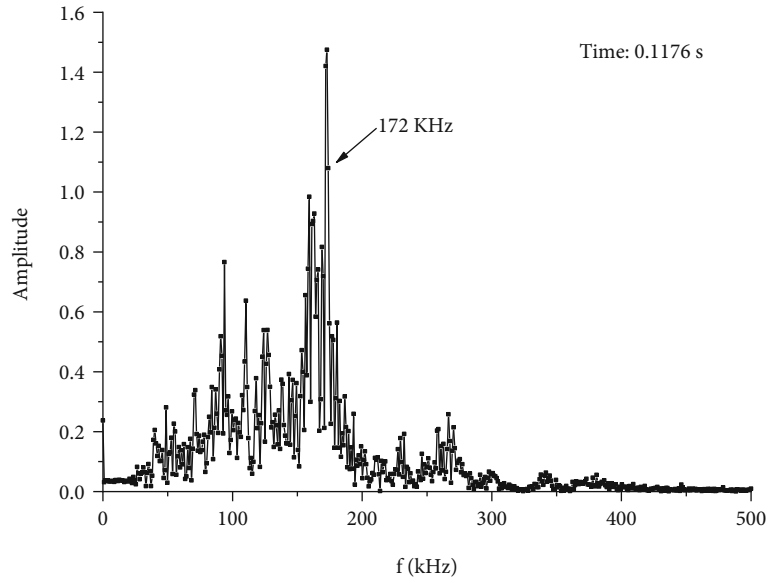

(a)

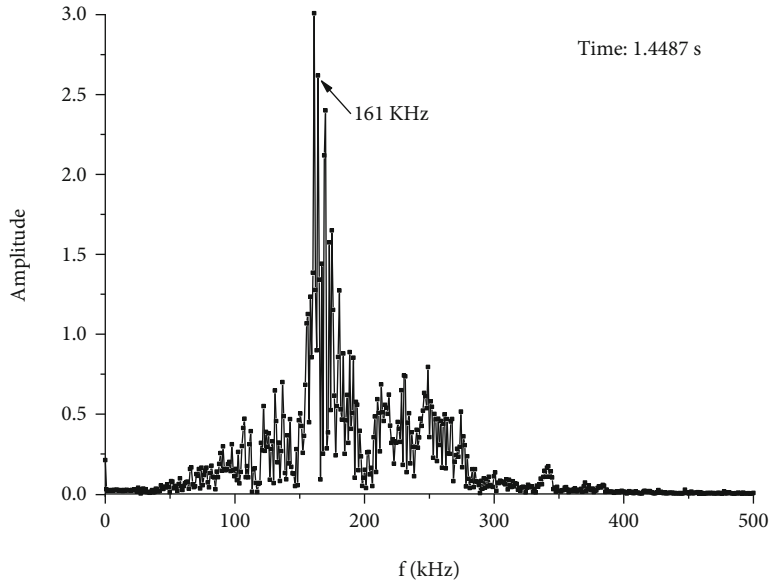

(b)

Figure 5: Continued.

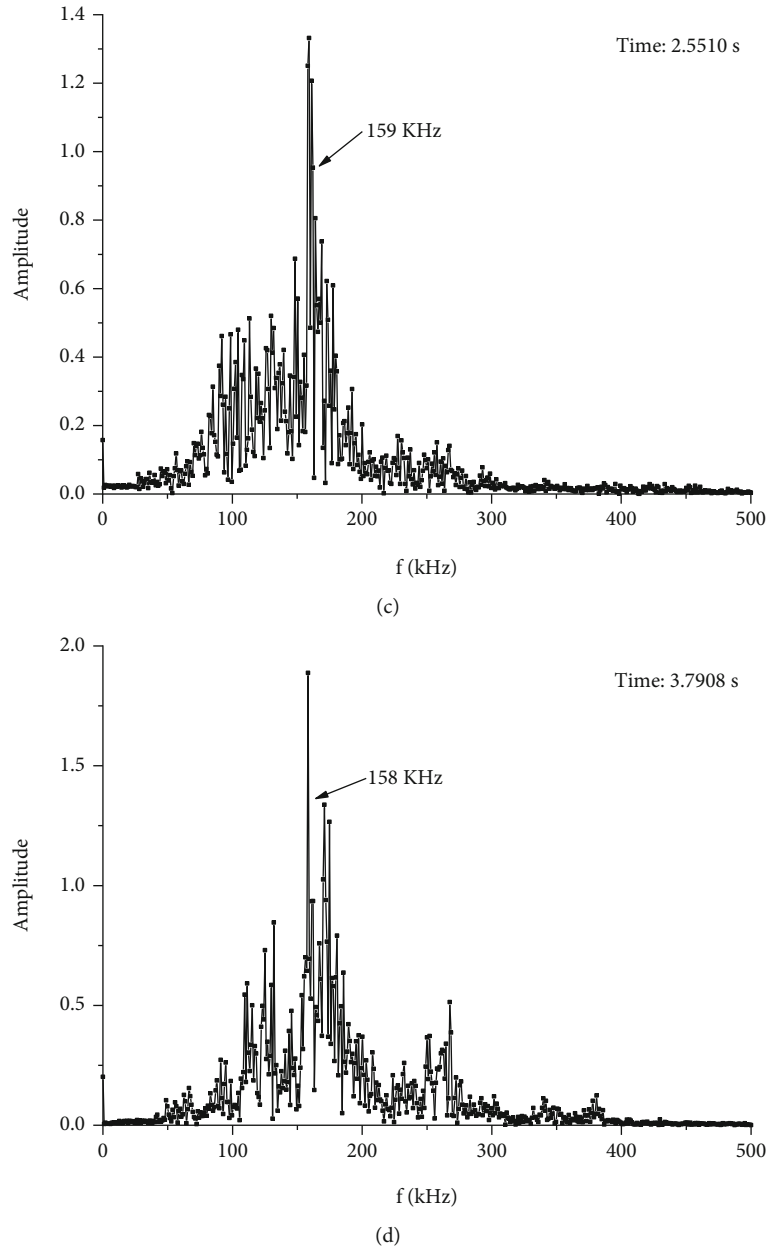

Figure 5: Waveform spectrogram of the waveform at the peak cutting force of H_2 coal.

with the foregoing, acoustic emissions have significant differences at different stages of cutting. In the compaction stage, the acoustic emission occurs at a higher density, and the D_t value is larger and has a decreasing trend. In the stable extrusion stage, acoustic emission appears the "relatively quiet period" and fractal dimension increases rapidly. In the bulk particle peeling stage, the number of acoustic emission occurrences increases sharply, and the D_t value reaches the maximum. Therefore, the acoustic emission during the cutting process has obvious periodic characteristics and can reflect the evolution process of the cutting force. In actual production, the coal cutting can be adjusted into a stable extrusion stage by the "relatively quiet period" of acoustic emission. At the same time, according to the change of D_t value, the trend of coal development to unstable structure is analyzed to predict the arrival of peak cutting force, and the cutting speed and traction speed of mining machinery are adjusted in time to avoid peak cutting force and reduce fatigue damage of equipment. It will improve the reliability of the coal machine.

4. Analysis of Acoustic Emission Waveform Characteristics at Peak Cutting Force

The acoustic emission signal in the process of coal cutting contains very rich information. Signal energy can respond to the cutting change along with the time, but it does not

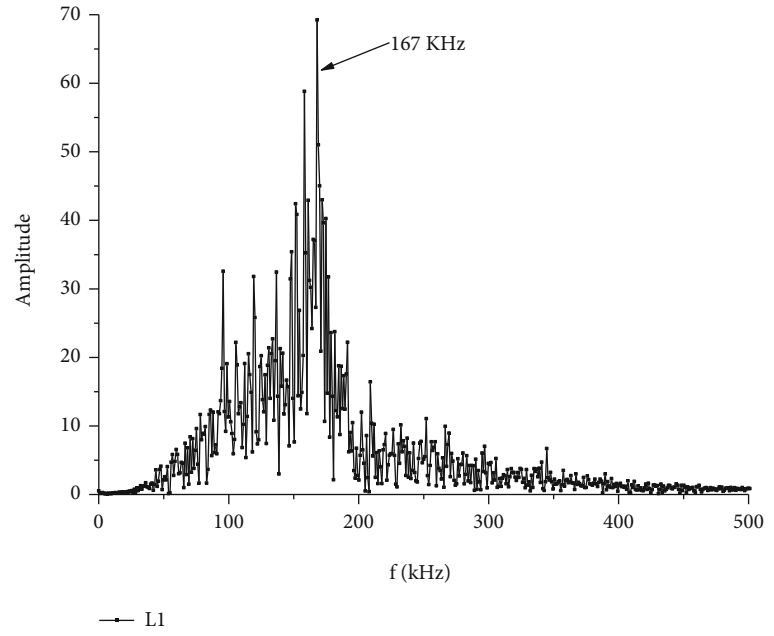

(a)

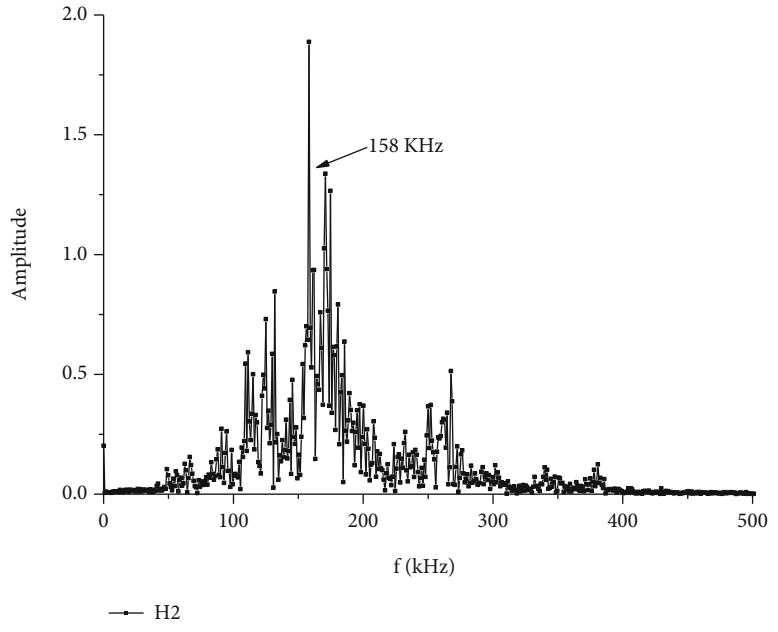

(b)

Figure 6: Continued.

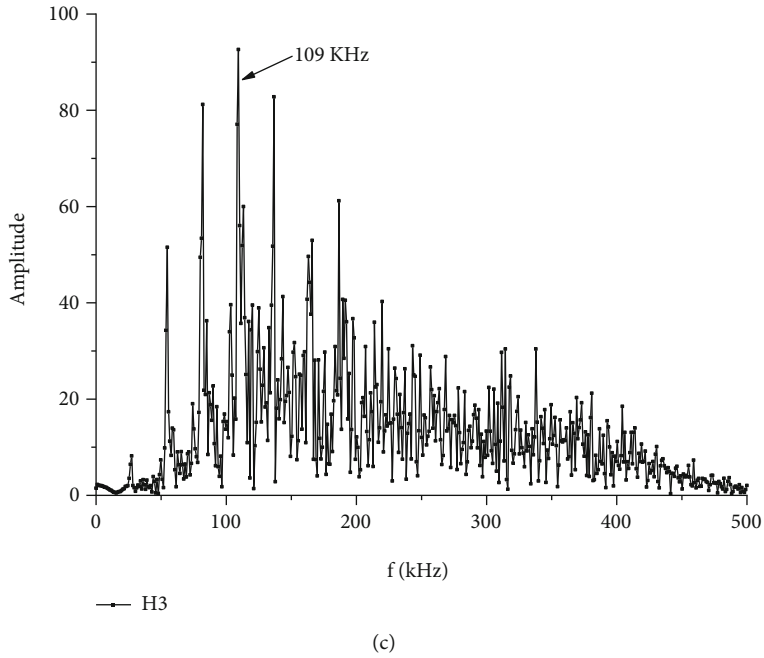

(c)

Figure 6: Waveform spectrogram of the maximum cutting force of different types of coal.

reflect the distribution of signal frequency. The analysis of the spectral characteristics of the signal helps to further clarify the acoustic emission characteristics of the coal cutting. The precursor of peak cutting force is analyzed in the previous papers, and now, the commonality of acoustic emission at different cutting peak forces is analyzed, in order to find the sign of peak cutting force.

4.1. Spectral Response Characteristics of Acoustic Emission Waveform at Peak Cutting Force. Acoustic emission monitors the elastic waves generated when the rock is destroyed. As an unsteady time-varying signal, it can obtain its frequency domain by fast Fourier transform (FFT) and extract the spectrum to obtain the frequency structure of the signal. In this paper, the acoustic emission signal waveforms at the peak cutting force of H_2 sample and the maximum cutting force of L_1, H_2, and H_3 are chronologically ordered. It is extracted and subjected to obtain the spectrum of acoustic emission signal using the FFT function in Matlab Time-Frequency Analysis Toolbox, as shown in Figures 5 and 6.

According to the literature [29], different types of rock damage have different time-frequency characteristics of acoustic emission. From Figure 5, the coal of the type H_2 has the same main frequency at the peak of the cutting force and is concentrated between 155 and 175 kHz, with a small difference, indicating that the type of failure at the peak cutting force during coal cutting is the same, which is mainly tensile failure [30]. Figure 6 depicts the time-frequency diagram of the different types of coal at the maximum cutting force. The main frequencies of L_1 and H_2 are 167 kHz and 158 kHz, respectively, and only have the main band; and H_3 has a dominant frequency of 109 kHz and has multiple main bands.

4.2. PSD Response Characteristics of Acoustic Emission Waveform at Peak Cutting Force. The cutting process is also a process of energy constantly changing in the coal body. The pick continuously inputs mechanical energy into the coal body, and the energy in the coal body continuously accumulates. When the coal storage limit is reached, the energy is suddenly released, resulting in a peak cutting force. The energy dissipation due to rock failure can be partially quantified by the AE energy [22]. Therefore, it can be seen that at the peak cutting force, that is, the turning point where the energy of the coal body evolves, the energy of the acoustic emission has a great significance. In this study, the Welch method has been used to calculate the PSD values of the AE signal. The PSD is a measure of the power (square root of the magnitude) in the frequency range of the signal [31]. As proposed by [22], the area enclosed by the PSD curve has been considered as a quantitative measure of the released energy of the recorded AE signal. In this paper, the acoustic emission signal waveforms at the peak cutting force of L_1, H_2, and H_3 samples are PSD calculated, and Figures 7(a) and 7(b) are obtained.

The PSD value of the acoustic emission waveform at different peak cutting forces during H_2 coal cutting is shown in Figure 7(a). Overall, H_2 coal has the same trend of change, which increases first and then decreases with frequency, indicating that the type of damage at peak cutting force is basically the same. Figure 7(b) shows the PSD values at the peak cutting forces of different coal rocks.

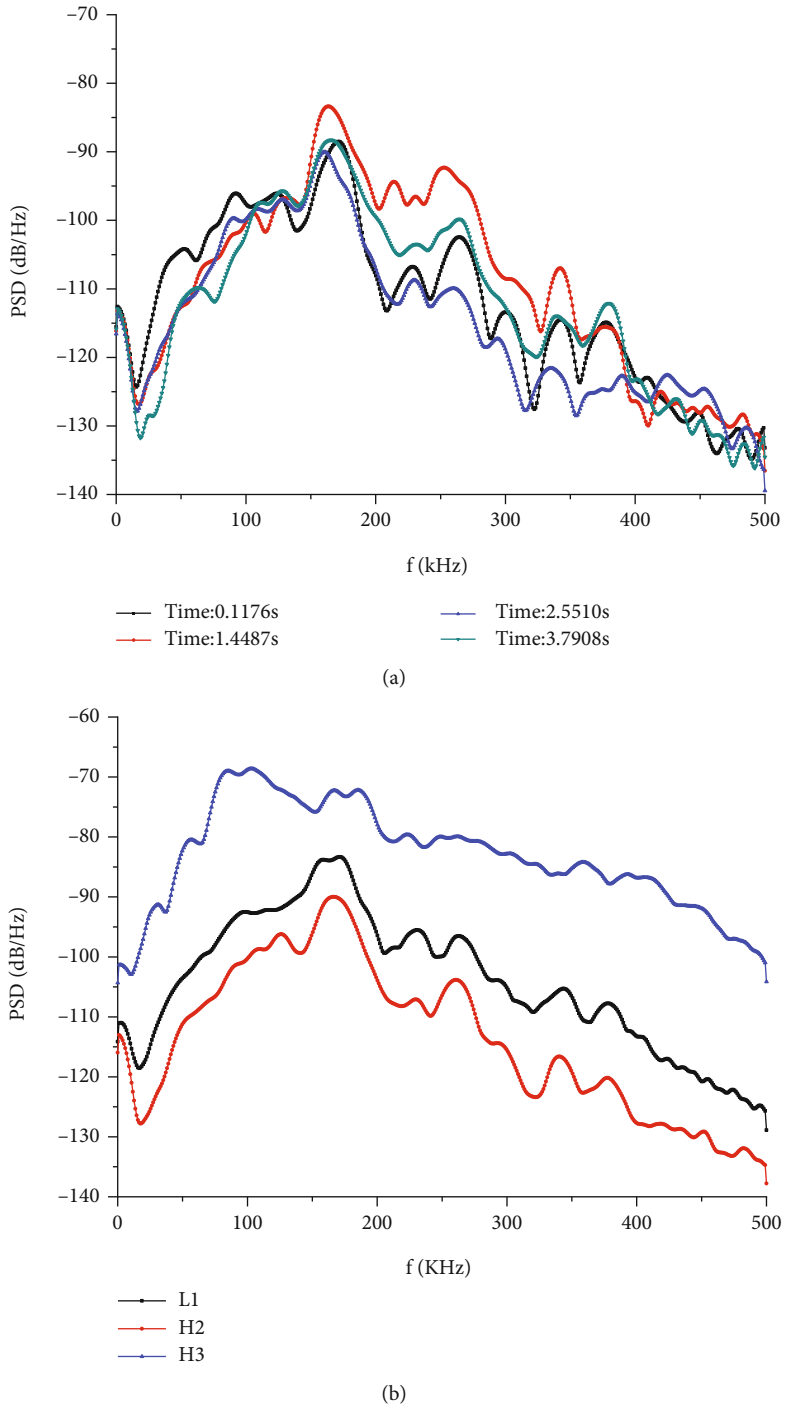

Figure 7: PSD characteristic curve: (a) PSD versus frequency at peak cutting force; (b) PSD versus frequency of three kinds of sample.

PSD peak H3 > L1 > H2, which is consistent with the time-frequency law. The integral calculation of the lower area of the PSD yields (Figures 8(a) and 8(b)). It can be seen that the area under the PSD curve at the peak cutting force of the H_2 sample is basically the same, and the differential coefficient is only 0.34%, indicating that the peak cutting force is consistently destroyed and the acoustic emission energy is consistent. At the same time, the area under the PSD curve of the three coals is shown in Figure 8(b). The area value is logarithmically related to the UCS of the coal sample. The larger the UCS is, the larger the area value is, and the larger the acoustic emission energy is. This is consistent with the increase of the energy required for rock failure with the increase of UCS.

In summary, the acoustic emission at the peak cutting force has the same frequency, the same PSD frequency spectrum, and the same PSD area value, indicating that the peak cutting force acoustic emission has commonality, and the commonality can be used for peak cutting force identification. At the same time, the acoustic emission at the peak

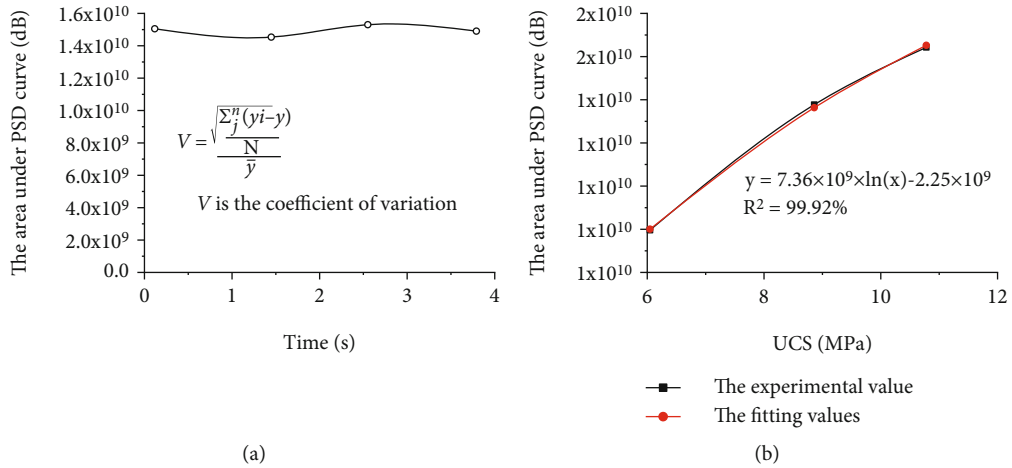

Figure 8: PSD curve integral area characteristic curve: (a) area under PSD curve at Peak Force; (b) area under PSD curve three kinds of sample.

cutting force has different characteristics in different coals. The acoustic emission frequency, PSD value, and PSD area value have different characteristics in different coals.

5. Conclusion

In underground excavation and drilling engineering, scholars paid more attention to the peak cutting force, while the time point of peak cutting force is ignored. Based on the analysis of the relationship between the cutting force and the acoustic emission during cutting process, the characteristics of the acoustic emission waveform at the peak cutting force are discussed, and the following beneficial conclusions are obtained:

Firstly, the evolution of acoustic emission energy can characterize the different stages of cutting. The cutting compaction stage is characterized by high energy density when the acoustic emission energy is large and the energy is small. When the acoustic emission is "relatively quiet," it is the cutting and compression stage. When the number of acoustic emission increases sharply and the energy is large, it is the size of the cutting block stripping stage.

Secondly, the time fractal dimension of the acoustic emission energy can reveal the stability of the coal structure. When the D_t value is stable, the fracture in the coal body is closed to the stable structure. When the D_t value rises, the crack in the coal body develops toward the unstable structure. The D_t value decline indicates that the coal body gradually develops to the stable structure after the large damage.

Thirdly, the acoustic emission waveforms at the peak cutting force of the same coal have the same characteristics, and different coals have different characteristics. The peak cutting force is not exactly the same in the same coal cutting, but the acoustic emission waveform at the peak cutting force has the same dominant frequency, the PSD has the same changing trend, and the common features of the area under the PSD are equal. Therefore, these parameters can be used as a sign of peak cutting force. The above common features have different performances in different coals, the waveforms have different PSD, and the area under the PSD curve is logarithmically related to UCS, which can be used as a sign to cut different coals.

Fourthly, acoustic emissions can predict the arrival of peak cutting forces. There are two major characteristics of the acoustic emission before the peak cutting force occurs: the "relatively quiet period" of the acoustic emission energy and the fractal dimension of the acoustic emission time increase rapidly. Therefore, the above characteristics are obtained, that is, the stable extrusion stage of the cutting is analyzed, and the peak cutting force can be predicted. At the same time, whether the cutting is subjected to the peak cutting force can be judged by the characteristics of the acoustic emission waveform.

Data Availability

The data used to support the findings of this study are available from the corresponding author upon request.

Conflicts of Interest

The authors declare that they have no conflicts of interest.

Acknowledgments

This research was supported by joint Ph.D. program of "double first rate" construction disciplines of CUMT.

References

[1] N. Bilgin, M. Demircin, H. Copur, C. Balci, H. Tuncdemir, and N. Akcin, "Dominant rock properties affecting the performance of conical picks and the comparison of some experimental and theoretical results," *International Journal of Rock Mechanics and Mining Sciences*, vol. 43, no. 1, pp. 139–156, 2006.

[2] G. Królczyk, M. Gajek, and S. Legutko, "Effect of the cutting parameters impact on tool life in duplex stainless steel turning process," *Tehnički Vjesnik*, vol. 20, pp. 587–592, 2013.

[3] H. Tuncdemir, N. Bilgin, H. Copur, and C. Balci, "Control of rock cutting efficiency by muck size," *International Journal of Rock Mechanics and Mining Sciences*, vol. 2, pp. 278–288, 2008.

[4] S. Dewangan and S. Chattopadhyaya, "Performance analysis of two different conical picks used in linear cutting operation of coal," *Arabian Journal for Science and Engineering*, vol. 41, no. 1, pp. 249–265, 2016.

[5] H. Kang, J.-W. Cho, J.-Y. Park et al., "A new linear cutting machine for assessing the rock-cutting performance of a pick cutter," *International Journal of Rock Mechanics and Mining Sciences*, vol. 88, pp. 129–136, 2016.

[6] P. L. Menezes, M. R. Lovell, I. V. Avdeev, J.-S. Lin, and C. F. Higgs III, "Studies on the formation of discontinuous chips during rock cutting using an explicit finite element model," *International Journal of Advanced Manufacturing Technology*, vol. 70, no. 1-4, pp. 635–648, 2014.

[7] O. Su and N. A. Akcin, "Numerical simulation of rock cutting using the discrete element method," *International Journal of Rock Mechanics and Mining Sciences*, vol. 48, no. 3, pp. 434–442, 2011.

[8] J. Liu, P. Cao, and K. Li, "A study on isotropic rock breaking with TBM cutters under different confining stresses," *Geotechnical and Geological Engineering*, vol. 33, no. 6, pp. 1379–1394, 2015.

[9] P. Samui, R. Kumar, and P. Kurup, "Determination of optimum tool for efficient rock cutting," *Geotechnical and Geological Engineering*, vol. 34, no. 4, pp. 1257–1265, 2016.

[10] I. Evans, "A theory of the cutting force for point-attack picks," *Geotechnical and Geological Engineering*, vol. 2, pp. 63–71, 1984.

[11] I. Evans, "Basic mechanics of the point-attack pick," *Colliery Guardian*, vol. 232, pp. 111–113, 1984.

[12] G. Kuidong, J. H. Du Changlong, and L. Songyong, "A theoretical model for predicting the Peak Cutting Force of conical picks," *Frattura ed Integrità Strutturale*, vol. 8, no. 27, pp. 43–52, 2014.

[13] Z. Qian-qian, H. Zhen-nan, Z. Meng-qi, and Z. Jian-guang, "Experimental study of breakage mechanisms of rock induced by a pick and associated cutter spacing optimization," *Rock and Soil Mechanics*, vol. 37, pp. 2172–2179, 2016.

[14] D. Niu, "Mechanical model of coal cutting," *International Journal of Rock Mechanics and Mining Sciences & Geomechanics Abstracts*, vol. 32, p. 169A, 1995.

[15] H. Jiang, C. Du, S. Liu, and Z. Liu, "Numerical analysis of rock cutting based on fracture mechanics," *Rock and Soil Mechanics*, vol. 34, pp. 1179–1184, 2013.

[16] L. Xuefeng, W. Shibo, G. Shirong, R. Malekian, and L. Zhixiong, "Investigation on the influence mechanism of rock brittleness on rock fragmentation and cutting performance by discrete element method," *Measurement*, vol. 113, pp. 120–130, 2018.

[17] X. Ma and D. Zhang, "Acoustic emission studies on rock cutting," *Chinese Journal of Rock Mechanics & Engineering*, vol. 15, no. 1, pp. 77–84, 1996.

[18] B. K. R. Prasad and R. V. Sagar, "Relationship between AE energy and fracture energy of plain concrete beams: experimental study," *Journal of Materials in Civil Engineering*, vol. 20, no. 3, pp. 212–220, 2008.

[19] A. I. Hassan, C. Chen, and R. Kovacevic, "On-line monitoring of depth of cut in AWJ cutting," *International Journal of Machine Tools and Manufacture*, vol. 44, no. 6, pp. 595–605, 2004.

[20] R. Kovacevic, H. Kwak, and R. Mohan, "Acoustic emission sensing as a tool for understanding the mechanisms of abrasive water jet drilling of difficult-to-machine materials," *Proceedings of the Institution of Mechanical Engineers, Part B: Journal of Engineering Manufacture*, vol. 212, no. 1, pp. 45–58, 1998.

[21] A. W. Momber, "Concrete failure due to air-water jet impingement," *Journal of Materials Science*, vol. 35, no. 11, pp. 2785–2789, 2000.

[22] R. Kovacevic, A. Momber, and R. Mohen, "Energy dissipation control in hydro-abrasive machining using quantitative acoustic emission," *The International Journal of Advanced Manufacturing Technology*, vol. 20, no. 6, pp. 397–406, 2002.

[23] M. Karakus and S. Perez, "Acoustic emission analysis for rock–bit interactions in impregnated diamond core drilling," *International Journal of Rock Mechanics and Mining Sciences*, vol. 68, pp. 36–43, 2014.

[24] Y. Xiao, C. Hurich, J. Molgaard, and S. D. Butt, "Investigation of active vibration drilling using acoustic emission and cutting size analysis," *Journal of Rock Mechanics and Geotechnical Engineering*, vol. 10, no. 2, pp. 390–401, 2018.

[25] C. U. Grosse and M. Ohtsu, *Acoustic Emission Testing*, Springer Science & Business Media, 2008.

[26] X.-T. Feng, "Introduction to intelligent rock mechanics," *Science*, 2000.

[27] X. G. Yin, S. L. Li, and H. Y. Tang, "Study on strength fractal features of acoustic emission in process of rock failure," *Chinese Journal of Rock Mechanics and Engineering*, vol. 24, pp. 3512–3516, 2005.

[28] G. Su, Y. Shi, X. Feng, J. Jiang, J. Zhang, and Q. Jiang, "True-triaxial experimental study of the evolutionary features of the acoustic emissions and sounds of rockburst processes," *Rock Mechanics and Rock Engineering*, vol. 51, no. 2, pp. 375–389, 2018.

[29] G. Su, Y. Shi, and X. Feng, "Acoustic signal characteristics in rock-burst process," *Chinese Journal of Rock Mechanics and Engineering*, vol. 35, pp. 1190–1201, 2016.

[30] X. Li, S. Wang, S. Ge, R. Malekian, and Z. Li, "Numerical simulation of rock fragmentation during cutting by conical picks under confining pressure," *Comptes Rendus Mecanique*, vol. 345, no. 12, pp. 890–902, 2017.

[31] P. Welch, "The use of fast Fourier transform for the estimation of power spectra: a method based on time averaging over short, modified periodograms," *IEEE Transactions on Audio and Electroacoustics*, vol. 15, no. 2, pp. 70–73, 1967.